Coupling schemes for atom–diatom interactions and an adiabatic decoupling treatment of rotational temperature effects on glory scattering

Vincenzo Aquilanti, Laura Beneventi, Gaia Grossi, and Franco Vecchiocattivi

Citation: The Journal of Chemical Physics **89**, 751 (1988); doi: 10.1063/1.455198
View online: http://dx.doi.org/10.1063/1.455198
View Table of Contents: http://scitation.aip.org/content/aip/journal/jcp/89/2?ver=pdfcov
Published by the AIP Publishing

Coupling schemes for atom–diatom interactions and an adiabatic decoupling treatment of rotational temperature effects on glory scattering

Vincenzo Aquilanti, Laura Beneventi, Gaia Grossi, and Franco Vecchiocattivi
Dipartimento di Chimica dell' Università, 06100 Perugia, Italy

(Received 28 January 1988; accepted 22 March 1988)

The quantum mechanical theory for scattering of a particle by a rigid rotor is formulated in five alternative diabatic representations, corresponding to alternative coupling schemes. Use is made of a recently introduced procedure for obtaining discrete representations by artificial quantization. In order to develop an efficient computational scheme for obtaining information on the interaction potential from atom–diatom scattering experiments, decoupling approximations are developed. An adiabatic representation in the coupled states framework is applied to the computation of integral cross sections and nonadiabatic coupling effects are analyzed. The approach provides an accurate description of the experimentally observed dependence of glory scattering from the rotational temperature of the diatom.

I. INTRODUCTION

This paper considers the quantum mechanics for the scattering of a particle from a rigid rotor as the usual model for the low energy interaction between an atom and a diatomic molecule. Most of our present knowledge of van der Waals interactions comes from atomic and molecular beam measurements of scattering cross sections.[1–5] In these experiments detailed information is obtained by the study of collisional interference effects, diffraction structure, and inelastic transitions which are sensitive to specific characteristics of the interaction between the colliding partners. A direct inversion procedure, which leads from scattering results to interatomic potential energy curves, has been attempted only in a few particularly favorable cases.[6] However, in most cases the scattering results are fitted by assumed potential energy functions in a trial and error procedure.

When for a given system in addition to scattering results other properties sensitive to the interaction are available, such as spectroscopic and thermophysical results, a combined analysis of all these experimental data can extend the range of validity of the potential energy function and can improve its reliability: several examples are available in the literature.[7–11]

The level of accuracy which can be obtained strongly depends on the theoretical scheme which is used to link the experimental observables to the interaction potential. While these procedures are well established for scattering by isotropic potentials, accurate full quantum mechanical calculations are often impractical when anisotropy is important, and approximations must be used.

The effect of anisotropy on molecular beam scattering was first observed as a quenching in the amplitude of glory undulations.[12,13] The quenching was first attributed to the coupling between vibrational modes and translational energy,[12] but it was afterwards established that a fundamental role is played by the angular dependence of the interaction potential[14,15] and therefore that the coupling between rotational and translational modes should be considered explicitly.

Actually, most recently, even very sophisticated molecular beam studies of atom—molecule collisions[16] have been given an admittedly preliminary interpretation by an approximation, the infinite order sudden (IOS), which recommends itself for its simplicity. One of the purposes of this paper is to show that in cases where IOS performs poorly it is possible to develop a scheme which allows relaxation of one of its most serious assumptions, namely that of an essential degeneracy of the rotational energy levels of the molecule.

From this laboratory, it has been argued that the dependence of the glory structure upon the rotational temperature of the diatom provides a clear experimental evidence for the failure of this energy sudden (ES) assumption.[8,9,17,18]

In the next section five alternative representations are considered for the present quantum mechanical problem: they lead to different quantum numbers according to different angular momentum coupling schemes. The discussion stresses the analogy between the present problem and the angular momentum analysis of open shell atom collisions, considered elsewhere.[19–22] The main decoupling approximations are then reviewed, in particular the relationship between IOS and the centrifugal sudden (CS) and energy sudden (ES) assumptions are stressed.

In Sec. III an adiabatic representation is introduced. Following previous experience on open shell atom collisions,[19–26] the adiabatic scheme is developed within the CS framework and shown to lead to a practical improvement with respect to IOS, especially when nonadiabatic coupling matrix elements are computed and their role assessed. Examples are also provided for the dependence of adiabatic states as a function of internuclear distance for typical interactions, such as those which describe the van der Waals forces between rare gas atoms and diatomic molecules. The behavior of these curves, and in particular the explicit consideration of nonadiabatic coupling terms, suggests the decoupling schemes to be used and defines their ranges of applicability.

The numerical example in Sec. IV illustrates the accuracy of this approach for the description of the energy depen-

 0021-9606/88/140751-11$02.10

dence of glory structure for a typical system. In particular, it provides the correct dependence on the rotational temperature of the diatom, information which appears not to be presently obtainable by different approaches of practical accessibility.

After a concluding section, the Appendix provides equations based on different perturbation schemes which should be useful in the implementation of this approach to the analysis of the data.

II. ATOM–DIATOM SCATTERING THEORY: ALTERNATIVE COUPLING SCHEMES AND DECOUPLING APPROXIMATIONS

The interaction potential $V(R,\vartheta)$ between a structureless atom A and a diatom molecule BC, when the vibrational degree of freedom is neglected, depends on R, the distance between A and the center of mass of the diatom, and on the orientation angle ϑ (see Fig. 1 for the definition of relevant quantities). The quantum mechanical theory of such a system has been extensively studied.[27] It is formulated as the scattering of a particle from a rigid rotor with a moment of inertia I. Its angular momentum j is combined with the orbital angular momentum of the atom–diatom system l to give the total angular momentum J with a component M along an axis fixed in space.

In order to describe the collision process, one has to solve, under scattering boundary conditions, a multichannel Schrödinger equation, at a fixed total angular momentum J and energy E:

$$\left\{\left(\frac{\hbar^2}{2\mu}\frac{d^2}{dR^2}+E\right)\mathbf{1}-\mathbf{V}^J(R)\right\}\mathbf{F}=0, \tag{1}$$

where the effective potential energy matrix $\mathbf{V}^J(R)$ is the representation of the sum of three operators:

$$\mathbf{V}^J(R)=\mathbf{V}_{\rm rot}+\mathbf{V}_{\rm centr}+\mathbf{V}_{\rm int}\,. \tag{2}$$

The first term in Eq. (2) is the Hamiltonian of the rotor

$$\mathbf{V}_{\rm rot}=\frac{\hbar^2}{2I}\mathbf{j}^2, \tag{3}$$

$\mathbf{V}_{\rm centr}$ is the centrifugal operator

$$\mathbf{V}_{\rm centr}=\frac{\hbar^2}{2\mu R^2}\mathbf{l}^2, \tag{4}$$

and $\mathbf{V}_{\rm int}$ is the scalar function $V(R,\vartheta)$.

Alternative representations in terms of different coupling schemes correspond to the possible choices of the relative role of these three terms. The following presentation stresses the analogy with the angular momentum coupling schemes analysis of the interaction of open shell atoms, analysis modeled on Hund's cases of the spectroscopy of rotating molecules.[19–21] As suggested previously, we use Greek letters to denote the five cases.[28]

A. Space fixed frame: Case (ϵ)

In the *laboratory* system of coordinates[27] the eigenfunctions of the molecule and of the atom are, respectively, the spherical harmonics $Y_{jm_j}(\hat{r})$ and $Y_{lm_l}(\hat{R})$, where (Fig. 1) $\hat{r}$ and $\hat{R}$ are the orientations of $\mathbf{r}$ and $\mathbf{R}$, and m_j and m_l are space fixed components of j and l, respectively. Since the potential is not spherically symmetric, neither l nor j are conserved during the collision; however an expansion of the total wave function in a set of functions where j and l are good quantum numbers is adequate in the asymptotic situation, where the potential goes to zero. Eigenfunctions of the total angular momentum J and of its projection M are obtained by vector coupling:

$$|JMjl\rangle=\mathscr{Y}_{jl}^{JM}(\hat{R},\hat{r})$$

$$=\sum_{m_j}\sum_{m_l}\langle jm_jlm_l|JM\rangle Y_{jm_j}(\hat{r})Y_{lm_l}(\hat{R}), \tag{5}$$

where $\langle jm_jlm_l|JM\rangle$ is a Clebsch–Gordan coefficient. From the asymptotic behavior of the radial functions $\mathbf{F}(R)$ in Eq. (1) at large R values it is possible to compute the scattering matrix and therefore all the observables. We designate the expansion in the set $|JMjl\rangle$ simply as the $|jl\rangle$ representation, or case (ϵ). Since the basis set of expansion (5) is given by eigenfunctions of $\mathbf{j}^2$ and $\mathbf{l}^2$, the first term in Eq. (2), namely the matrix representation of the angular momentum operator of the rotor [Eq. (3)] results to be diagonal with the eigenvalues $Bj(j+1)$, where B is the rotational constant, $B=\hbar^2/2I$. In the same way the second term in Eq. (2), namely the centrifugal operator [Eq. (4)] in matrix notation, is diagonal with eigenvalues $l(l+1)/2\mu R^2$. The interaction potential matrix $V(R,\vartheta)$ in this $|jl\rangle$ representation is not diagonal and its off-diagonal elements:

$$\langle jlJ|V|j'l'J\rangle=\int\int\mathscr{Y}_{jl}^{JM}V\mathscr{Y}_{j'l'}^{JM}\,d\hat{R}\,d\hat{r} \tag{6}$$

are the coupling terms in Eq. (1). Therefore, in this $|jl\rangle$ representation, the channel coupling in Eq. (1) is due exclusively to the interaction potential (see Table I).

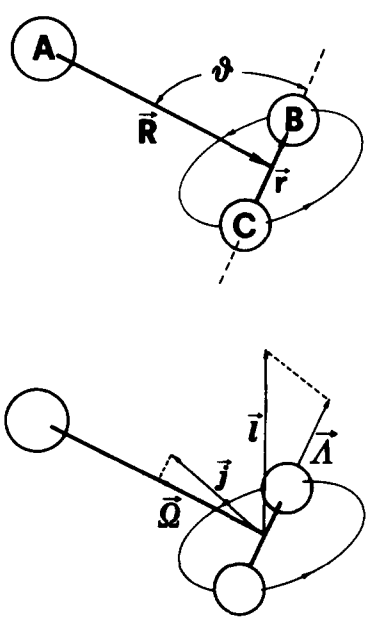

FIG. 1. The schemes illustrate the definition of Jacobi vectors and angular momenta for the atom A interacting with the molecule BC. When vibrations in the latter are considered frozen (r = constant), the interaction potential depends only on R and ϑ. The rotational and orbital angular momenta $\mathbf{j}$ and $\mathbf{l}$ are associated to the $\mathbf{r}$ and $\mathbf{R}$ vectors, respectively. Projections of $\mathbf{j}$ on R and of $\mathbf{l}$ on r are also shown. Because of the parity conservation, we can consider only the absolute value of projections, $0\leqslant\Omega\leqslant j$, $0\leqslant\Lambda\leqslant l$.

TABLE I. Summary of properties of alternative diabatic representations.

Coupling case	Representation[a]	Matrix elements[b] V_{int}	V_{rot}	V_{centr}
(ϵ)	$\|jl\rangle$	full j and l coupling	diagonal	diagonal
(γ)	$\|j\Omega\rangle$	full j coupling	diagonal	tridiagonal in Ω
(δ)	$\|l\Lambda\rangle$	full l coupling	tridiagonal in Λ	diagonal
(α)	$\|Nn\Omega\rangle$	diagonal	full n coupling	tridiagonal in Ω
(β)	$\|Nn\Lambda\rangle$	diagonal	tridiagonal in Λ	full n coupling

[a] See Figs. 1 and 2. All representations are also eigenfunctions of the total angular momentum J, its space fixed projection M, and a parity quantum number $\epsilon = +1$ or -1.
[b] In the comparison with Table I of Ref. 21, note that properties of spin–orbit matrix elements for Hund's cases (b) and (d) were inadvertently interchanged; similarly for centrifugal matrix elements for cases (c) and (d).

B. Body fixed frames: Cases (γ) and (δ)

Next we consider a frame transformation from the space fixed system to body fixed systems (Fig. 1). If we choose **r** as a quantization axis, the j component along this axis, j_r, is zero, while the corresponding **l** component, l_r, will be labeled by Λ. Then the projection of **J** along **r** is

$$J_r = l_r = \Lambda.$$

On the other hand, if we choose R as the quantization axis, the **l** component along this axis vanishes while the component of **j** is Ω and thus

$$J_R = j_R = \Omega.$$

We can therefore use two alternative bases, $|j\Omega\rangle$ and $|l\Lambda\rangle$, to expand the scattering total wave function; their elements are eigenfunctions of j and its projection along R, and of l and its projection along r, respectively. Both have been considered in the literature.[29,30]

The $|jl\rangle$, $|j\Omega\rangle$, and $|l\Lambda\rangle$ representations are related one to each other by orthogonal transformations: specifically, the transformation between $|jl\rangle$ [Eq. (5)] and $|j\Omega\rangle$ is[29]

$$|jl\rangle = \sum_{l} \frac{1+\epsilon(-)^{J-l}}{[2(1+\delta_{\Omega 0})]^{1/2}} (-)^{J-\Omega} \times \langle j\Omega, J-\Omega | l0\rangle |j-\Omega\rangle, \quad (7)$$

where the parity number ϵ can take the two alternative values $\epsilon = +1$ or $\epsilon = -1$.

In the $|j\Omega\rangle$ representation, the first term in Eq. (2), which represents the molecular rotational interaction [Eq. (3)] is still diagonal, while couplings are introduced in the second term of Eq. (2) for $\Omega \neq \Omega'$, whose matrix elements are now

$$\begin{aligned}\langle j\Omega|l^2|j\Omega'\rangle &= [2\Omega^2 - J(J+1) - j(j+1)] \quad \text{for } \Omega = \Omega' \\ &= [J(J+1) - \Omega(\Omega \pm 1)]^{1/2}[j(j+1) - \Omega(\Omega \pm 1)]^{1/2} \quad \text{for } \Omega' = \Omega \pm 1\end{aligned} \quad (8)$$

and in the interaction potential matrix which is diagonal in Ω but couples states with $j \neq j'$. This matrix will be explicitly given and used in the next section.

On the contrary in the $|l\Lambda\rangle$ representation the angular momentum operator of the orbital motion is still diagonal, the molecular rotation matrix is diagonal in l and couples states with $\Lambda = \Lambda \pm 1$ (all the relevant matrix elements for the $|l\Lambda\rangle$ case can be obtained from the ones for the previous case interchanging both j and l, and Ω and Λ). The interaction potential matrix is now diagonal in Λ and couples states with $l' = l$. Therefore, choosing different bases to expand the scattering wave function one obtains sets of equations of the same dimensionality but with a different structure. It is appropriate to designate the $|j\Omega\rangle$ and $|l\Lambda\rangle$ representations as the (γ) and (δ) cases,[28] respectively (see also Table I).

C. Discrete representations: Cases (α) and (β)

Representations for which the potential matrix is diagonal [such as Hund's cases (a) and (b) in the open shell atom–atom problem] have been introduced only recently[28] for the present problem where the interaction is a continuous function of the angle ϑ between Jacobi vectors (Fig. 1), so the treatment requires a discretization procedure.[31] Our recipe[28] starts by establishing a connection between cutting the angular range ($0 \leqslant \vartheta < \pi$) in N slices and introducing an arti-

ficial vector A of length $[A(A+1)]^{1/2}$ putting $A = N/2$, and interpreting the integers n which count the slices ($-N/2 \leqslant n \leqslant N/2$) as projection quantum numbers (see Fig. 2), we can exploit angular momentum algebra at its full power. The consequence will be that expressions representing Eq. (6) will be replaced by a summation.

This is due to the fact that the basic tools of the method are the discrete analogs of spherical harmonics, which are essentially Clebsch–Gordan coefficients. It is therefore possible to obtain a finite basis analog of a given representation, e.g., an $|Nj\Omega\rangle$ representation, which tends to the $|j\Omega\rangle$ of case (γ) as N goes to infinity.[28] For the present application, we derive the explicit expression for the transformation between the $|j\Omega\rangle$ representation of case (γ) and the discrete representation of case (α) which we denote $|Nn\Omega\rangle$:

$$|Nn\Omega\rangle = \sum_{j=0}^{N} \frac{1-\epsilon(-)^{N/2-j}}{[2(1+\delta_{n_0})]^{1/2}} \cdot (-)^{N/2-n+j} \times \left\langle \frac{N}{2} - (n+\Omega), \frac{N}{2}\, n | j\Omega \right\rangle |Nj\Omega\rangle , \tag{9}$$

where the parity number ϵ can take the two alternative values $\epsilon = +1$ or $\epsilon = -1$.

It is straightforward to obtain the matrix elements for the molecular rotational and the centrifugal operators. While those for the latter now couple channels having different n and Ω, those for the molecular rotational interaction couple only states with different n and have a very simple close form expression:

$$\langle Nn\Omega | j^2 | Nn'\Omega \rangle = N\left(\frac{N}{2}+1\right) - 2n^2 \quad \text{for } n = n'$$
$$= -(1+\delta_{n_0})\left[\frac{N}{2}\left(\frac{N}{2}+1\right) - n(n+1)\right] \quad \text{for } n' = n \pm 1, \tag{10}$$

which we will use later. The potential matrix is diagonal in this case. Explicitly, its elements are the discretized values of the potential function $V(R,\vartheta_n)$ computed at angles given by the formula

$$\cos\vartheta_n = -\frac{2n}{[N(N+2)]^{1/2}} \simeq -\frac{2n}{N} \quad \text{for large } N. \tag{11}$$

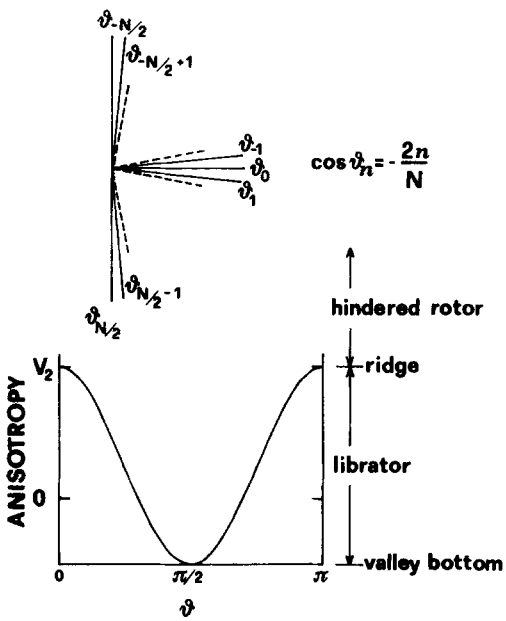

FIG. 2. The upper scheme illustrates the discretization in N slices (conveniently taken to be even) of the angular range $0 \leqslant \vartheta < \pi$ (see Ref. 28). The label n, which plays the role of an artificial quantum number, varies in the range from $-N/2$ to $N/2$. Because of symmetry, only the range $0 \leqslant n \leqslant N/2$ will be considered in the present application. The lower scheme shows a typical angular dependence for the anisotropic part of the potential for the interaction between an atom and a homonuclear diatomic molecule. The case $V_2 > 0$, corresponding to a lower energy for the T-shaped configuration with respect to the collinear one is considered. The classification of the modes are also indicated.

Along the same lines it is possible to introduce a case (β) and a representation $|Nn\Lambda\rangle$, the role of l and j (and that of Λ and Ω) being interchanged with respect to case (α). The diagonal form seen above for the potential is preserved: it can be argued that this property will make cases (α) and (β) particularly useful at short range when potential effect overwhelm molecular rotational and centrifugal ones. In analogy with the open shell atom–atom problem, case (α) will be preferred when molecular rotational effects are more important than centrifugal ones, and case (β) vice versa. Table I summarizes the properties of the five coupling schemes.

D. The CS, ES, and IOS decoupling approximations

A main problem for the routine solution of the full set of coupled equations typically arises from the large amount of channels needed to obtain converged scattering matrix elements. Decoupling approximations leading to a reduction to the number of coupled equations are therefore welcome. Again our discussion will exploit the analogy with the open shell atom–atom collision theory.[20,21]

The CS approximation has been extensively studied in the last years: In some recent developments it is referred to as *coupled states* approximation,[32] while when independently introduced by Pack[33] it has been called *centrifugal sudden* approximation. In the earlier literature, it was referred to as the j_z-conserving approximation: in the language of the present paper it corresponds to conservation of the quantum number Ω.

To obtain the CS decoupling scheme, one introduces an effective value $\bar{l}$ for the orbital angular momentum and the centrifugal potential [Eq. (4)] in the Hamiltonian is approximated as follows:

$$\frac{\hbar^2}{2\mu R^2}\mathbf{l}^2 \simeq \frac{\hbar^2 \bar{l}(\bar{l}+1)}{2\mu R^2}\mathbf{1}. \tag{12}$$

This leads to remarkable consequences in the coupled equations in either the case (γ) or the case (α) representations (see Table I). In fact being the centrifugal matrix now diagonal, in case (γ), only states with different j values are now coupled by the interaction potential; in case (α), the coupling is only in the molecular rotational term where channels with neighboring n values are coupled.

In the *energy sudden* (ES)[34–36] approximation, the matrix representation of the molecular rotational operator [Eq. (3)] is similarly replaced by a diagonal matrix obtained by defining an *average molecular rotational* eigenvalue $\bar{j}$ and working in case (δ) or in case (β) representations,

$$\frac{\hbar^2}{2I}\mathbf{j}^2 \simeq B\bar{j}(\bar{j}+1)\mathbf{1}. \tag{13}$$

This implies that Λ, the l component along the quantization axis $\mathbf{r}$ (Fig. 1), is assumed to be conserved. Since in case (δ) the centrifugal matrix is diagonal, in this representation the channel coupling is given only by the potential matrix which couples states with different l values. In case (β) where the interaction potential matrix is diagonal, the coupling is due only to the centrifugal term, where only channels with the neighboring n values are coupled.

This decoupling scheme implies the drastic assumption of an essential degeneracy of molecular rotation states. However, being the centrifugal operator represented correctly, this approach is in a sense complementary to the CS approximation.

The *infinite order sudden* (IOS) approximation[37] follows from the combined use of both the ES and the CS assumptions. In our approach Eqs. (12) and (13) are both substituted in the Hamiltonian (2) and representations for the cases (α) or (β) are used. Thus, the Schrödinger equation in the IOS approximation depends on ϑ only through $V(R,\vartheta)$, and can be solved for specific values of ϑ as a parameter. Actually, our derivation is rather restrictive as far as the choice of the grids of angles ϑ_n [Eq. (11)] is concerned. It has been shown[31] that values dictated by any convenient quadrature procedure can be exploited. Procedures to obtain scattering observables for the full anisotropic system from single channel potential scattering computations at each angle are well established and extensively used.

III. ADIABATIC CORRELATION OF STATES

The diabatic representations (and the decoupling approximations) seen above are linked by orthogonal transformations [such as those in Eqs. (7) and (9)] which are R independent and diagonalize only part of the full interaction $\mathbf{V}^J(R)$ in Eq. (2) (see Table I). In this section we introduce an *adiabatic* representation, where an R-dependent transformation simultaneously diagonalizes the molecular rotational and the interaction potential, $\mathbf{V}_{rot}$ and $\mathbf{V}_{int}$, contributions to the matrix $\mathbf{V}(R)$. In this way a correlation is obtained between the short range (interaction potential dominant) and the long range (j and l good quantum numbers) behavior.

A. Limiting cases

Restricting our discussion to the coupled states approach [see Eq. (12)], where the centrifugal term is diagonal by assumption, it is interesting to study how the relative importance of the two terms $\mathbf{V}_{rot}$ and $\mathbf{V}_{int}$ in Eq. (2) varies as a function of the distance R for an atom interacting with a homonuclear diatomic molecule (Fig. 1). Qualitatively, at long range the system can be described as a free rotor weakly interacting with the atom through an effectively spherically symmetric potential $V_0(R)$, while at short range the atom is bound to the molecule and oscillates around the most stable configuration, which very often is the perpendicular one ($\vartheta = \pi/2$). For this last case we call $V_\perp$ the relevant interaction [$V_\perp(R) = V(R,\pi/2)$]. These two limiting situations and the correlation between them can be illustrated most simply assuming that the potential $V(R,\vartheta)$ is expanded in a series of Legendre polynomials truncated at the second term:

$$V(R,\vartheta) = V_0(R) + V_2(R)P_2(\cos\vartheta), \tag{14}$$

where

$$P_2(\cos\vartheta) = (3\cos^2\vartheta - 1)/2 \tag{15}$$

(when this assumption is not valid, the details of the following developments will have to be slightly modified, but the qualitative features will remain unchanged). Since

$$V_2 = 2(V_0 - V_\perp)$$

and defining $V_\parallel(R) = V(R,0)$ one has

$$V_\parallel = V_0 + V_2 = 3V_0 - 2V_\perp.$$

When $V_2 > 0$, the anisotropic part of the potential $V_2P_2(\cos\vartheta)$ as a function of ϑ has a minimum value $-V_2/2$ when $\vartheta = \pi/2$ and two maxima, V_2 high, when $\vartheta = 0$ and π (see Fig. 2). Therefore, in the potential energy surface in the R,ϑ plane, one can identify[38] a line connecting the minima as a function of R (*valley bottom*, $V_\perp = V_0 - V_2/2$) and a line connecting the maxima (*ridge*, $V_\parallel = V_0 + V_2$) (for negative V_2 we have the opposite situation; see also Fig. 3). The potential below the valley bottom is energetically forbidden, but below and above the ridge we can distinguish two situations. At constant R we have below the ridge bound states oscillating in a well, while above the ridge we have hindered rotor states (Fig. 2). Correspondingly, at short range, where V_2 is large and positive, the system has oscillatory modes around the minimum at $\vartheta = \pi/2$. At long range V_2 becomes negligible with respect to V_0 and we have an almost freely rotating diatom, which interacts with the atom mainly through V_0, the anisotropic term being only a weak perturbation. Formulas from perturbation theory for the situations both above and below the ridge are given in the Appendix. They fail at ridge, where explicit inclusion of nonadiabatic coupling and a numerical approach are required.

B. Adiabatic correlation and nonadiabatic coupling

The equivalent of Eq. (1) in the adiabatic representation is

$$\left[-(\hbar^2/2\mu)\left[\mathbf{1}\frac{d}{dR} + \mathbf{P}(R)\right]^2 + \boldsymbol{\epsilon}(R)\right]\mathbf{F}_a = E\mathbf{1}\mathbf{F}_a. \tag{16}$$

The diagonal matrix $\boldsymbol{\epsilon}$ contains the eigenvalues of $\mathbf{V}_{int}$ and

$\mathbf{V}_{rot}$ (of course independent of the diabatic representation chosen):

$$\mathbf{T}(R)[\mathbf{V}_{int}(R)+\mathbf{V}_{rot}(R)]\tilde{T}(R)=\epsilon(R). \tag{17}$$

These eigenvalues are effective potential energy curves in the adiabatic representation. The coupling between them is represented by the matrix **P**, which is related to the orthogonal diagonalizing matrix **T** by

$$\mathbf{P}(R)=\frac{d\mathbf{T}(R)}{dR}\cdot\tilde{T}(R). \tag{18}$$

The simultaneous diagonalization of the $\mathbf{V}_{rot}$ [Eq. (4)] and $\mathbf{V}_{int}$ operators can be most easily effected in the $|j,\Omega\rangle$ representation of case (γ): matrix elements can be written

$$M^{\Omega}_{jj'}(R)=j(j+1)+\frac{1}{B}\langle j\Omega Vj'\Omega\rangle . \tag{19}$$

When the truncated expansion (11) for the potential is assumed, the matrix element $\langle j\Omega Vj'\Omega\rangle$ becomes

$$\begin{aligned}\langle j\Omega Vj'\Omega\rangle &= V_0(R)+V_2(R)\int_0^{\pi}Y^{*}_{j\Omega}(\vartheta,0)\\ &\quad\times Y_{j'\Omega}(\vartheta,0)P_2(\cos\vartheta)\sin\vartheta\,d\vartheta\\ &= V_0(R)\delta_{jj'}+V_2(R)\langle j2\Omega0|j'\Omega\rangle\\ &\quad\times\langle j200|j'0\rangle\left(\frac{2j+1}{2j'+1}\right)^{1/2},\end{aligned} \tag{20}$$

and therefore expression (19) becomes

$$M^{\Omega}_{jj'}=j(j+1)+\left(\frac{2j+1}{2j'+1}\right)^{1/2}\times\langle j2\Omega0|j'\Omega\rangle\langle j200|j'0\rangle\frac{V_2}{B}. \tag{21}$$

One obtains a tridiagonal simmetric matrix which couples the $j=j'\pm2$ states. Replacing the Clebsch–Gordan coefficients with their explicit expression, the generic matrix elements as a function of j, Ω, and V_2/B can be obtained:

$$\begin{aligned}M^{\Omega}_{jj}&=j(j+1)+\frac{j(j+1)-3\Omega^2}{(2j+3)(2j-1)}\frac{V_2}{B}+\frac{V_0}{B},\\ M^{\Omega}_{j,j+2}&=\frac{3[(j-\Omega+2)(j-\Omega+1)(j+\Omega+2)(j+\Omega+1)]^{1/2}}{2(2j+3)[(2j+5)(2j+1)]^{1/2}}.\end{aligned} \tag{22}$$

This matrix has been diagonalized by a truncation to a 40×40 dimension (which amounts to the inclusion of the first $20\,j$ levels) and for V_2/B values between -300 and 300. Several adiabatic states for $\Omega=0$ are reported in Fig. 3

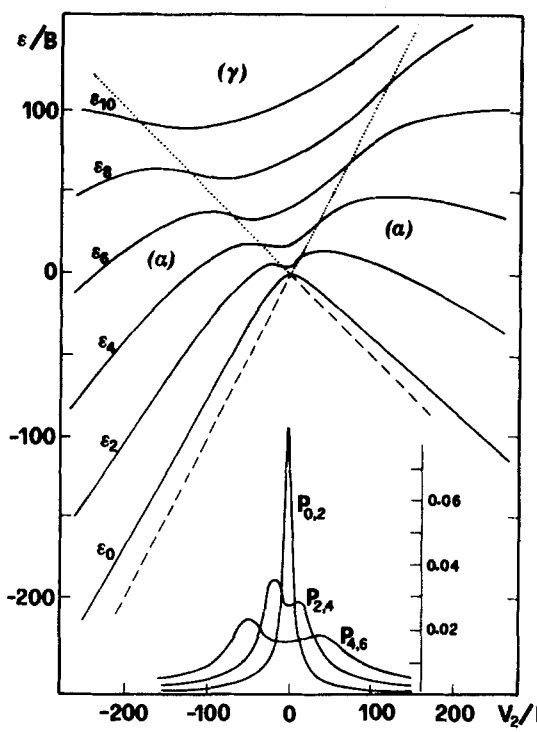

FIG. 3. Plots in reduced units of the dependence from anisotropy of adiabatic states and nonadiabatic couplings. The dotted and dashed straight lines V_2/B and $-V_2/2B$ represent ridges and valley bottoms, respectively, and exchange their roles for positive and negative values of V_2.

as a function of V_2. Also reported in the figure are the shape of the largest P matrix elements which describe the nonadiabatic couplings between the adiabatic states. They were obtained in two ways from the computed diagonalizing matrix **T** [Eq. (17)]; either directly from Eq. (18) by two diagonalizations at close R values, X and $X+\Delta X$, where $X=V_2/B$:

$$\mathbf{P}(X)=(\Delta X)^{-1}[\tilde{\mathbf{T}}(X)\mathbf{T}(X+\Delta X)-\mathbf{1}] \tag{23}$$

or more efficiently from the formula

$$P_{ij}(X)=[\epsilon_i(X)-\epsilon_j(X)]^{-1}[\tilde{\mathbf{T}}(X)\mathbf{M}'(X)\mathbf{T}(X)], \tag{24}$$

where $\mathbf{M}'=d\mathbf{M}/dX$, which follows from the Hellmann–Feynman theorem and requires only a single diagonalization for each R value. For the relatively small size of this problem, the two procedures are essentially equivalent. It is evident from Fig. 3 that the maxima of the **P** matrix elements tend to peak at the ridge.

An alternative procedure starts from the case (α) representation $|Nn\Omega\rangle$ (Table I). In this basis, following Ref. 28 it can be shown that the matrix to be diagonalized is now:

$$\begin{aligned}M_{nn}&=N\left(\frac{N}{2}+1\right)-2n^2+V(r,\vartheta_n),\\ M_{nn'}&=-(1+\delta_{n_0})\left[\frac{N}{2}\left(\frac{N}{2}+1\right)-nn'\right]\quad n'=n\pm1.\end{aligned} \tag{25}$$

For the present simple problem the diagonalization procedure converged very fast to the adiabatic eigenvalue as the dimension of the matrix was increased to the number of slices N of about 10 (this gave an eigenvalue problem of the same size than before). Both procedures gave identical results with minimal effort. The advantage of the discretiza-

tion procedure is obvious when $V(R,\vartheta)$ does not have the simple form of Eq. (11), because then it avoids the computation of the matrix element integrals.

This approach is similar to the one used for studying the interaction of open shell atoms with rare gases from molecular beam results.[22–25] Scattering was described by effective adiabatic curves, and the nonadiabatic coupling between them was shown to be negligible. Similar recipes have been proposed for strong interactions between ions and polar molecules.[39]

C. Adiabatic states and couplings for He–N_2 and Ar–N_2

We now proceed to construct explicitly the adiabatic states, as the eigenenergies generated by simultaneous numerical diagonalization of $\mathbf{V}_{rot}$ and $\mathbf{V}_{int}$ for specific systems. These states can be labeled as $|j\Omega\rangle$, since case (γ) holds asymptotically, and the nonadiabatic couplings are generated within the same computation using Eq. (24). Typical results are shown in Fig. 4 for the He–N_2 and Ar–N_2 systems. For He–N_2, the potential energy surface obtained by a recent multiproperty analysis has been used.[11] For the Ar–N_2 case, rather than using a potential of similar reliability,[9] a model interaction has been used instead,[40] because for this interaction extensive numerical experience exists. In particular, for this Ar–N_2 model system an assessment has been recently presented of the validity of CS and IOS approximations for the glory scattering.[41]

From plots such as those in Fig. 4 it is possible to identify at once which channels are effective in a given scattering experiment, which of these channels can be considered effectively decoupled, and which nonadiabatic coupling between states has to be considered explicitly. It is the latter feature which dominates inelastic effects.

IV. THE GLORY EFFECT AND ITS DEPENDENCE ON ROTATIONAL TEMPERATURE

Since its first experimental observation[42] the glory interference effect in the collision velocity dependence of integral cross sections has been studied extensively. When the collision partners show anisotropy of interaction the glory undulations appear modified with respect to those produced by isotropically interacting partners. Such a modification consists of a damping and a shifting of the undulatory structure and has been observed for many open shell atom–atom[22–25,43] and atom–molecule systems.[12–15,44] Much work has been also devoted to characterize theoretically these anisotropy effects in order to connect the glory modifications with the anisotropy of interaction. In this context, early classical mechanics studies[45] first checked *ante litteram*, the IOS (at the time called fixed angle approximations) and other assumptions. Distorted wave and approximations of the sudden type were also investigated[46] prior to the explicit introduction of the angular momentum decoupling schemes reviewed in Sec. II. Experimentally, the role on glory of an-

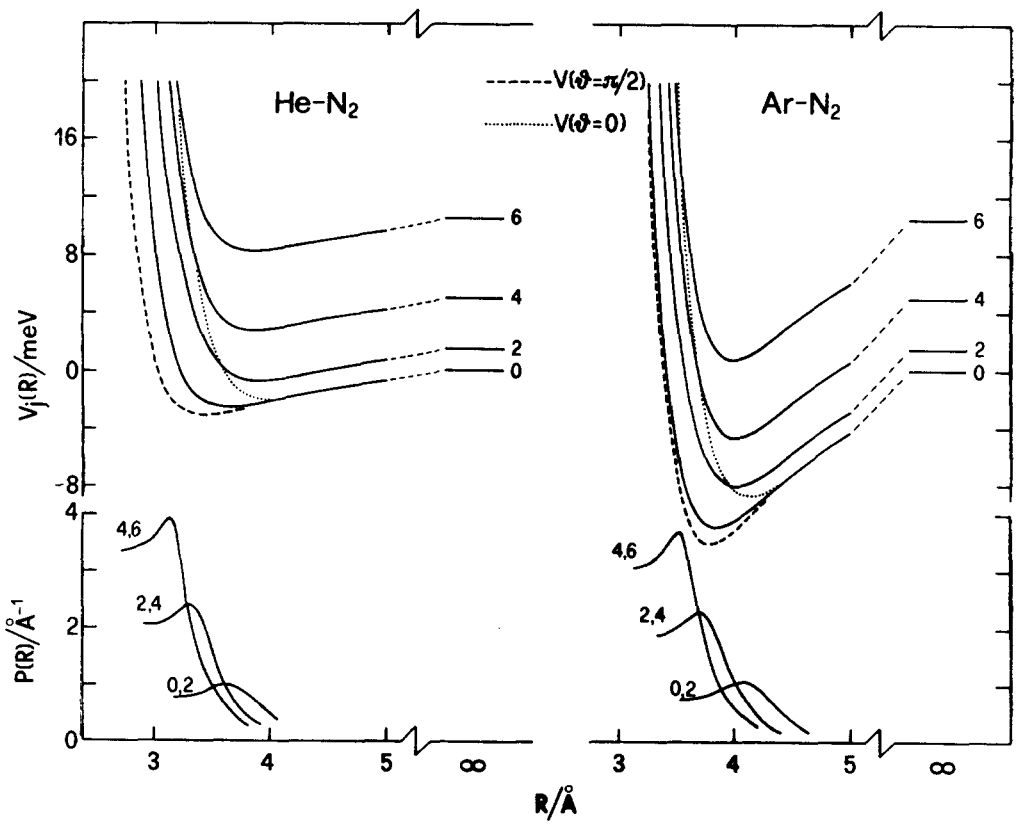

FIG. 4. In the upper parts, adiabatic energy curves are shown, obtained as described in the text, for $\Omega = 0$. Also shown are the $V(\vartheta = 0)$ and the $V(\vartheta = \pi/2)$ curves, which represent the ridge and valley bottom lines for these potential energy surfaces. States have essentially the character of librating modes below the ridge and of a hindered rotor above it. In the lower parts, nonadiabatic coupling matrix elements are shown. They are obtained directly from those in Fig. 3 by using $\mathbf{P}(R) = \mathbf{P}(X)dX/dR$ which follows from Eq. (23). As expected from experience on a variety of other physical situations, such couplings peak where the adiabatic curves cross the ridge.

isotropy has been extensively probed in Nijmegen.[47] Recently in our laboratory[8,9,17,18] a dependence of the glory amplitude on the rotational temperature of the diatom has also been observed for O_2 and N_2 scattered by Ar and Kr. In this section we apply the adiabatic analysis developed in Sec. III to a discussion of this effect which cannot be described by IOS. Specifically we consider the Ar–N_2 system, for which only even rotational states are coupled to the ground state and will be considered in the following.

A. Adiabatic potentials and nonadiabatic couplings for Ar–N_2

Since the glory structure in integral cross sections is mainly sensitive to features of the wells,[48,49] it is clear from Fig. 4 that for the description of the glory effect most curves can be considered adiabatically decoupled, but that nonadiabatic coupling has to be introduced explicitly for the lowest states.

Connor, Clary, and Sun,[41] in their calculation for the glory effect for the Ar–N_2 system have shown that CS and IOS both agree with exact results in the 500 to 3500 m/s velocity range, introducing $j=0$ as the only entrance channel. We succeeded in reproducing their results within mutual numerical errors by including in the scattering calculation only the lowest $j=0$ and 2 states, and properly combining them by explicitly computing the effect of nonadiabatic coupling. Interestingly the type of coupling between states will turn out to be of the perturbed resonance type first described by Rosen and Zener.[50]

In fact the nature of nonadiabatic couplings is specified by the analytic properties of the adiabatic energy levels and of the elements of the P matrix in the neighborhood of maxima for the latter (in the present case and in many other problems the regions of interest are concentrated astride of the potential ridge[38]). If we focus our attention on two levels and on the matrix element which couples them, then the Nikitin exponential model[51] is sufficiently general to cover all the interesting cases, ranging between a true avoided crossing situation (first studied by Landau, Zener, and Stuckelberg[52]), and a perturbated symmetric resonance (as studied by Rosen and Zener,[50] Demkov and others[53]). A characteristic parameter α in Nikitin's approach depends on the ratio between the energy difference at infinite separation $\Delta\epsilon_\infty$, and at the maximum R^* in the matrix element for nonadiabatic coupling, $\Delta\epsilon(R^*)$:

$$\alpha = 2 \arcsin \Delta\epsilon(R^*)/2\Delta\epsilon_\infty . \tag{26}$$

Specifically (see Fig. 4), for the interaction between the ϵ_{00} and ϵ_{20} states, we have $\Delta\epsilon_\infty = 1.485$ and $\Delta\epsilon(R^*) = 2.161$ meV, where $P_{02}(R^*) = 1.07\times10^8$ cm^{-1}. From Eq. (26) we have $\alpha \simeq \pi/2$, i.e., very close to the perturbed symmetric resonance case. Accordingly, the transition probability is given by the Demkov formula[53] for perturbed resonance, which is therefore shown to be accurate for this situation. The radial velocity at R^* and the glory impact parameter were computed by usual formulas.[49]

The results of such computations are exhibited in Fig. 5: the comparison with IOS shows perfect agreement at high collision energy, the discrepancy at low energy being due to the failure of the IOS assumption of degenerate rotor states, which is not made in our approach. At low collision energy our results show that, because of the lower efficiency of nonadiabatic effects, the system evolves mainly along the lowest adiabatic curve and the quenching of the glory structure decreases.

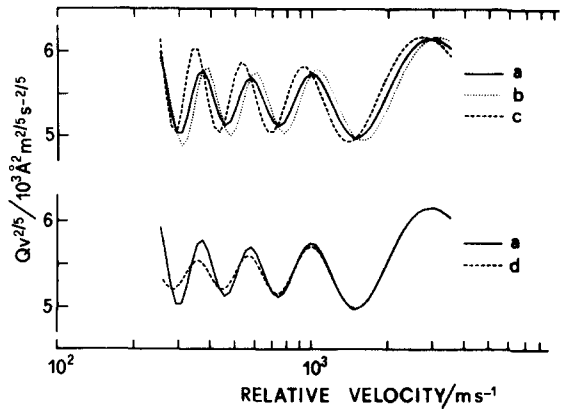

FIG. 5. The glory structure (entrance channel $j=0$) for the model Ar–N_2 system obtained by the present two state adiabatic approach with nonadiabatic coupling [curves (a)]. Curves (b) and (c) show the glory scattering from adiabatic curves correlating with the rotor states $j=0$ and $j=2$, respectively. They give curve (a) when combined as described in the text. Curve (d) is the IOS result. The perfect agreement at higher velocities deteriorates at lower velocities where the IOS assumption of degenerate rotor states becomes incorrect.

B. Integral cross sections for Ar–N_2

The present approach makes it feasible the computation of integral cross sections as a function of relative velocity at different values for the initial rotational angular momentum of the diatomic molecule. These results can in turn be combined to give finally the dependence of the glory pattern as a function of the rotational temperature. In Fig. 6(a) integral cross sections for different initial rotational states are reported, while in Fig. 6(b) the cross sections for different rotational temperatures of the diatomic molecule are shown as obtained by Boltzmann averaging. The states included in the computation for the highest rotational temperature are the even ones from $j=0$ to $j=44$, and all their projections Ω from 0 to 44. This computation was made possible by implementing to this problem a fast and accurate procedure for obtaining the glory cross sections.[49] In agreement with experimental observation[8,9,17,18] the glory structure so calculated appear to be partially damped at low rotational temperature and the damping decreases when the rotational temperature increases.

V. CONCLUSIONS

In this paper we have provided a unifying formulation of alternative representations for the quantum mechanical theory of scattering from an anisotropic potential. The theory is of interest for the analysis of low energy collisions of atoms from diatomic molecules. For the treatment of these experi-

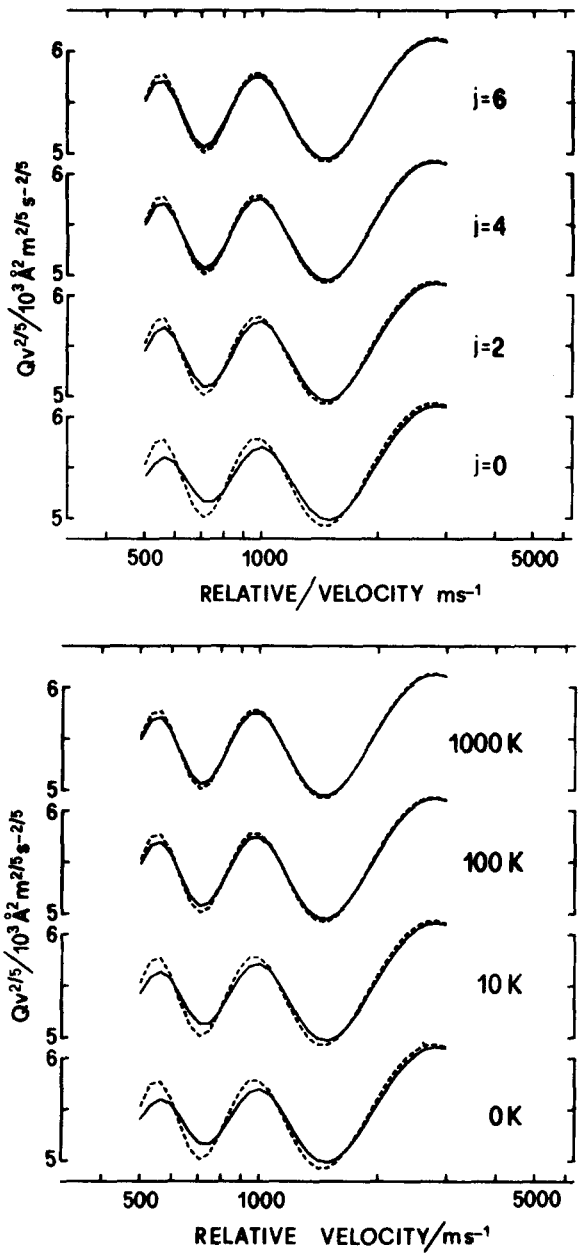

FIG. 6. Effect of initial rotational states (a) and of the initial rotational temperature (b) of the N_2 molecule on the glory structure for the model Ar–N_2 system, obtained as described in the text: The dashed curve, representing the glory structure from the isotropic potential V_0, is repeated on each graph for comparison and shows that the effects of the anisotropy decrease the higher is the rotational angular momentum of the diatomic molecule.

ments an adiabatic formulation is also provided and tested. The results show that the effect of the rotational temperature on the glory undulations is in the same direction as indicated by the experimental observations. They also indicate that the present approach represents an accurate computational route for extracting information on the potentials from the modification of the glory structure induced by anisotropy.

Further analytical and computational work should confirm the practical use of this approach, in particular, semianalytical formulas based on the theory of perturbed librators below the ridge and perturbed rotors above the ridge are available for the construction of adiabatic curves (see the Appendix). The theory can be also implemented for nonzero electronic angular momenta, such as for collisions involving NO molecules.[54–56] The extension of the present approach to differential total and inelastic cross sections and to the computation of transport properties is also being pursued.

APPENDIX: PERTURBATION FORMULAS ABOVE AND BELOW THE RIDGE

The adiabatic eigenvalues as a function of the anisotropic part of the interaction potential $X = V_2/B$ as calculated in the text and plotted in Fig. 3 are of general validity for a potential surface as in Eq. (14). When multiplied by B, they represent the adiabatic corrections to be added to the spherical interaction $V_0(R)$ for different j values and as a function of R to obtain the channel states as, e.g., those in Fig. 4.

Both for analyzing the qualitative character of these curves and for the practical implementation of this approach, it is interesting to observe that the asymptotic behavior of the $\epsilon_{j\Omega}/B$ levels can be described by perturbation theory of the rigid rotor and harmonic oscillator equations. The rigid rotor levels are simply given by

$$\epsilon_{j\Omega} = Bj(j+1) \tag{A1}$$

and this is the limit when V_2 vanishes, in particular for $R \to \infty$. With reference to Fig. 2, we have harmonic oscillations in the bottom of the well for V_2 large and positive. We have from Eq. (16),

$$\tfrac{1}{2}(3\cos^2\vartheta - 1) = \tfrac{1}{2}(3\sin^2\zeta - 1), \tag{A2}$$

where $\zeta = \vartheta - \pi/2$; one can consider $\sin^2\zeta \simeq \zeta^2$ around $\vartheta = \pi/2$. Replacing $V(\zeta) = (\zeta^2 - 1)/2$ in the Schrödinger equation of the harmonic oscillator, one obtains its levels

$$\frac{\epsilon_v}{B}(X) = -\frac{X}{2} + \left(v + \frac{1}{2}\right)\sqrt{6X}. \tag{A3}$$

This expression gives curves in rather good agreement with the exact ones[54] for very large values of V_2, i.e., for small range.

In order to improve on Eq. (A1) and to obtain an increase in the range of validity also for moderate values of X, it is useful to record the following results from the second order perturbation theory[54]:

$$E_{j\Omega}(X) = j(j+1) + \frac{j(j+1) - 3\Omega^2}{(2j+3)(2j+1)}X + \frac{9}{8(2j+1)}\left[\frac{(j^2-\Omega^2)(j-\Omega-1)(j+\Omega-1)}{(2j-1)^2(2j-3)}\right.$$
$$\left. - \frac{(j-\Omega+2)(j-\Omega+1)(j+\Omega+2)(j+\Omega+1)}{(2j+3)^3(2j+5)}\right]X^2 + O(X^3). \tag{A4}$$

To improve on Eq. (A3) for the description of the behavior at large V_2 an expression has been obtained by considering the complete operator $\mathbf{V}_{\rm rot} + \mathbf{V}(R,\vartheta)$ and from its diagonalization by using the $|n\rangle$ basis of the harmonic oscillator. The $\mathbf{V}_{\rm rot}$ operator depends on ϑ but also on Ω and therefore the levels so obtained depend on n but also on Ω. The following expression is obtained:

$$\frac{\epsilon_{v,\Omega}}{B}(X) = -\frac{X}{2} + \left(v+\frac{1}{2}\right)\sqrt{6X} - \frac{1}{4}(2v^2+2v+3) + \left(\frac{2}{3X}\right)^{1/2}\left(v+\frac{1}{2}\right)\left(\Omega^2-\frac{1}{4}\right) + \Omega^2 + O(X^{-1}). \quad \text{(A5)}$$

A detailed comparison shows that Eqs. (A4) and (A5) describe very well the system except in the region just around the ridge where both expressions diverge.

[1] H. Pauly, in *Atom–Molecule Collision Theory: A Guide for the Experimentalist*, edited by R. B. Bernstein (Plenum, New York, 1979), p. 111.
[2] G. Scoles, Annu. Rev. Phys. Chem. **31**, 81 (1980).
[3] U. Buck, Comments At. Mol. Phys. **17**, 143 (1986).
[4] F. Vecchiocattivi, Comments At. Mol. Phys. **17**, 163 (1986).
[5] M. Faubel, Adv. At. Mol. Phys. **19**, 345 (1983).
[6] R. B. Gerber, Comments At. Mol. Phys. **17**, 65 (1985).
[7] R. A. Aziz, in *Inert Gases*, edited by M. L. Klein (Springer, Berlin, 1984), and references therein.
[8] F. Pirani and F. Vecchiocattivi, Chem. Phys. **59**, 387 (1981).
[9] R. Candori, F. Pirani, and F. Vecchiocattivi, Chem. Phys. Lett. **102**, 412 (1983); J. Chem. Phys. **84**, 4833 (1986).
[10] M. Keil and J. A. Parker, J. Chem. Phys. **82**, 1947 (1985).
[11] F. A. Gianturco, M. Venanzi, R. Candori, F. Pirani, F. Vecchiocattivi, A. S. Dickinson, and M. S. Lee, Chem. Phys. **109**, 417 (1986).
[12] E. A. Gislason and G. H. Kwei, J. Chem. Phys. **46**, 2838 (1967); H. L. Kramer and P. R. LeBreton, *ibid.* **47**, 3367 (1967).
[13] R. K. B. Helbing and E. W. Rothe, J. Chem. Phys. **48**, 3945 (1968); E. W. Rothe and R. K. B. Helbing, *ibid.* **50**, 3945 (1969).
[14] P. R. LeBreton and H. L. Kramer, J. Chem. Phys. **51**, 3627 (1969).
[15] R. K. B. Helbing. J. Chem. Phys. **51**, 3628 (1969).
[16] M. Keil, J. T. Slankas, and A. Kuppermann, J. Chem. Phys. **70**, 541 (1979); J. T. Slankas, M. Keil, and A. Kuppermann, *ibid.* **70**, 1482 (1979); U. Buck, F. Huisken, J. Schleusener, and H. Pauly, Phys. Rev. Lett. **38**, 690 (1977); U. Buck, F. Huisken, J. Schleusener, and J. Schaefer, J. Chem. Phys. **72**, 1512 (1980); J. Andres, U. Buck, F. Huisken, J. Schleusener, and F. Torello, *ibid.* **73**, 5620 (1980); U. Buck, Faraday Discuss. Chem. Soc. **73**, 187 (1982); U. Buck, F. Huisken, G. Maneke, and J. Schaefer, J. Chem. Phys. **78**, 4430 (1983); U. Buck, F. Huisken, A. Kholhase, D. Otten, and J. Schaefer, *ibid.* **78**, 4439 (1983); U. Buck, H. Meyer, and R. J. LeRoy, *ibid.* **80**, 5589 (1984); M. Faubel, K. H. Kohl, and J. P. Toennies, *ibid.* **73**, 2506 (1980); M. Faubel, K. H. Kohl, J. P. Toennies, K. T. Tang, and Y. Y. Yang, Faraday Discuss. Chem. Soc. **73**, 205 (1982); M. Faubel, K. H. Kohl, J. P. Toennies, and F. A. Gianturco, J. Chem. Phys. **78**, 5629 (1983).
[17] F. Pirani, F. Vecchiocattivi, J. J. H. van den Biesen, and C. J. N. van den Meijdenberg, J. Chem. Phys. **75**, 1042 (1981).
[18] G. Liuti, E. Luzzatti, F. Pirani, and G. G. Volpi, Chem. Phys. Lett. **121**, 559 (1985).
[19] V. Aquilanti and G. Grossi, J. Chem. Phys. **73**, 1165 (1980).
[20] V. Aquilanti, P. Casavecchia, G. Grossi, and A. Laganá, J. Chem. Phys. **73**, 1173 (1980).
[21] V. Aquilanti, G. Grossi, and A. Laganá, Nuovo Cimento B **63**, 7 (1981).
[22] V. Aquilanti, F. Pirani, and F. Vecchiocattivi, in *Structure and Dynamics of Weakly Bound Complexes*, edited by A. Weber (Reidel, Dordrecht, 1987), p. 423.
[23] V. Aquilanti, E. Luzzatti, F. Pirani, and G. G. Volpi, J. Chem. Phys. **73**, 1181 (1980).
[24] V. Aquilanti, E. Luzzatti, F. Pirani, and G. G. Volpi, Chem. Phys. Lett. **90**, 382 (1982).
[25] V. Aquilanti, G. Grossi, and F. Pirani, in *Electronic and Atomic Collisions*, edited by J. Eichler, I. V. Hertel, and N. Stolterfoht (North-Holland, Amsterdam, 1983), p. 441.
[26] A. Aguilar, B. Brunetti, S. Rosi, F. Vecchiocattivi, and G. G. Volpi, J. Chem. Phys. **82**, 773 (1985).
[27] A. M. Arthurs and A. Dalgarno, Proc. R. Soc. London Ser. A **256**, 540 (1960); see *Atom–Molecule Collision Theory: A Guide for the Experimentalist*, edited by R. B. Bernstein (Plenum, New York, 1979), especially chapters by S. Stolte and J. Reuss, J. C. Light, D. J. Kouri, and D. Secrest.
[28] V. Aquilanti and G. Grossi, Lett. Nuovo Cimento **42**, 157 (1985). In the implementation of the theory given in this reference, we explicitly introduced the parity factors appropriate for the present problem.
[29] R. B. Walker and J. C. Light, Chem. Phys. **7**, 84 (1975); J. M. Launay, J. Phys. B **9**, 1823 (1976); compare also the transformation between cases (e) and (c) in the open shell atom–atom problem (Ref. 19).
[30] E. S. Chang and U. Fano, Phys. Rev. A **6**, 173 (1972).
[31] An alternative discretization procedure based on quadrature formulas has been introduced and applied successfully to several atom–molecule scattering successfully to several atom–molecule scattering problems by Light and co-workers: see, for example, J. V. Lill, G. A. Parker, and J. C. Light, J. Chem. Phys. **85**, 900 (1986); see also R. J. Cross, Jr., *ibid.* **85**, 3268 (1986).
[32] P. McGuire and D. J. Kouri, J. Chem. Phys. **60**, 2488 (1974).
[33] R. T Pack, J. Chem. Phys. **60**, 633 (1974).
[34] S. I. Chu and A. Dalgarno, Proc. R. Soc. London Ser. A **342**, 191 (1975).
[35] D. Secrest, J. Chem. Phys. **62**, 710 (1975).
[36] V. Khare, J. Chem. Phys. **68**, 4631 (1978).
[37] This very popular approximation has been described, applied, and assessed by many authors. See, for example, Ref. 5 and the book quoted in Ref. 27. See also G. A. Parker and R. T Pack, J. Chem. Phys. **68**, 1585 (1978); A. S. Dickinson, Comp. Phys. Commun. **17**, 51 (1979); F. A. Gianturco and A. Palma, J. Phys. B **18**, L519 (1985); M. Bowers, M. Faubel, and K. T. Tang, J. Chem. Phys. **87**, 5687 (1987); P. Casavecchia, L. Beneventi, F. Vecchiocattivi, G. G. Volpi, D. Lemoine, and M. H. Alexander, J. Chem. Phys. (to be published).
[38] For the verification and the analysis of the role of the ridges in the potential in *reactive* processes, see, for example, V. Aquilanti, in *Theory of Chemical Reaction Dynamics*, edited by D. C. Clary (Reidel, Dordrecht, 1986), p. 383; V. Aquilanti, S. Cavalli, and G. Grossi, Chem. Phys. Lett. **133**, 531 (1987); V. Aquilanti and S. Cavalli, *ibid.* **133**, 538 (1987); **141**, 309 (1987), and in a more general context, see V. Aquilanti, S. Cavalli, and G. Grossi, in *Chaotic Behaviour in Quantum Systems*, edited by G. Casati (Plenum, New York, 1985), p. 299; Chem. Phys. Lett. **43**, 110 (1984), and references therein.
[39] K. Takayanagi, Comments At. Mol. Phys. **9**, 143 (1980); *XII ICPEAC, Abstracts of Contributed Papers*, edited by S. Datz (Gatlinburg, TN, 1981), p. 921.
[40] M. D. Pattengill, R. A. LaBudde, R. B. Bernstein, and C. F. Curtiss, J. Chem. Phys. **55**, 5517 (1971).
[41] J. N. Connor, D. C. Clary, and H. Sun, Mol. Phys. **49**, 1139 (1983).
[42] E. W. Rothe, P. K. Rol, S. M. Trujillo, and R. H. Neynaber, Phys. Rev. **128**, 659 (1962).
[43] V. Aquilanti, G. Liuti, F. Pirani, F. Vecchiocattivi, and G. G. Volpi, J. Chem. Phys. **65**, 4751 (1976).
[44] R. K. B. Helbing and E. W Rothe, J. Chem. Phys. **50**, 3531 (1969); **53**, 1555 (1970); **53**, 2501 (1970); E. Richman and L. Wharton, *ibid.* **53**, 945 (1970); P. M. Dehmer and L. Wharton. *ibid.* **61**, 4264 (1974).
[45] R. J. Cross and D. R. Herschbach, J. Chem. Phys. **43**, 3530 (1965).
[46] R. J. Cross, J. Chem. Phys. **46**, 609 (1967); R. E. Olson and R. B. Bernstein, *ibid.* **49**, 162 (1968); R. J. Cross, *ibid.* **49**, 1976 (1968); R. E. Olson and R. B. Bernstein, *ibid.* **50**, 246 (1969); C. F. Curtiss and R. B. Bernstein, *ibid.* **50**, 1168 (1969); W. H. Miller, *ibid.* **50**, 3124 (1969); W. H. Miller, *ibid.* **50**, 3410 (1969); W. H. Miller, *ibid.* **50**, 3868 (1969); R. J. Cross, *ibid.* **52**, 5703 (1970); see also R. J. Cross, *ibid.* **83**, 5536 (1985).
[47] J. Reuss and S. Stolte, Physica **42**, 111 (1969); S. Stolte, J. Reuss, and H. L. Schwartz, *ibid.* **57**, 254 (1972); H. L. Schwartz, S. Stolte, and J. Reuss, Chem. Phys. **2**, 1 (1973); W. Frassen and J. Reuss, Physica **63**, 313 (1973); J. W. Kuijpers and J. Reuss, Chem. Phys. **4**, 277 (1974); L. Zandee, J. Veberne, and J. Reuss, *ibid.* **26**, 1 (1977); L. Zandee and J. Reuss, *ibid.* **26**, 327 (1977); **26**, 345 (1977); D. Klaassen, H. Thuis, S. Stolte, and J. Reuss, *ibid.* **27**, 107 (1978).
[48] R. B. Bernstein, J. Chem. Phys. **37**, 1880 (1963); **37**, 2599 (1963); R. B. Bernstein and T. J. P. O'Brien, Discuss. Faraday Soc. **40**, 35 (1965); J. Chem. Phys. **46**, 1208 (1967); E. F. Greene and E. A. Mason, *ibid.* **57**, 2065 (1972); R. B. Bernstein and R. A. LaBudde, *ibid.* **58**, 1109 (1973); E. F. Greene and E. A. Mason, *ibid.* **59**, 2651 (1973).

[49]F. Pirani and F. Vecchiocattivi, Mol. Phys. **45**, 1003 (1982).
[50]N. Rosen and C. Zener, Phys. Rev. **40**, 502 (1932).
[51]E. E. Nikitin, Discuss. Faraday Soc. **33**, 14 (1962); E. E. Nikitin, Adv. Quantum Chem. **5**, 135 (1970); J. E. Bayfield, E. E. Nikitin, and A. I. Reznikov, Chem. Phys. Lett. **19**, 471 (1973).
[52]L. D. Landau, Phys. Z. Sowietunion **2**, 46 (1932); C. Zener, Proc. R. Soc. London Ser. A **137**, 696 (1932); E. C. G. Stuckelberg, Helv. Phys. Acta **5**, 369 (1932).
[53]Yu. N. Demkov, Sov. Phys. JETP **45**, 195 (1963); see also M. S. Child, in *Atom–Molecule Collision Theory: A Guide for the Experimentalist,* edited by R. B. Bernstein (Plenum, New York, 1979), p. 427.
[54]L. Beneventi, Tesi di Laurea in Chimica, Universitá di Perugia, 1985.
[55]For recent experiments on scattering of rare gases by NO molecules, see P. Casavecchia, A. Laganá, and G. G. Volpi, Chem. Phys. Lett. **112**, 445 (1984); L. Beneventi, P. Casavecchia, and G. G. Volpi, J. Chem. Phys. **85**, 7011 (1986).
[56]B. Pouilly and M. H. Alexander, J. Chem. Phys. **88**, 3581 (1988), propose a similar analysis for the scattering of CaF ($A\ ^2\Pi$) by rare gases.